

# SAR optimization for multi-dipole antenna array with regard to local hyperthermia

**Abstract.** The following paper describes the valid optimization problem of multi-element circular array that contains 16 equal-length dipole antennas surrounding given two-spherical object. The task of the authors was to maximize the specific absorption rate (SAR) inside the inner object, while maintaining its minimum value in the external sphere. The proposed approach includes changes in the powers and phases of the voltage sources supplying individual dipoles of the antenna matrix. The shown method may have huge impact in localized tumor heating during thermal therapy.

**Streszczenie.** Niniejsza praca opisuje ważny problem optymalizacji wieloelementowego szyku kołowego, który zawiera 16 anten dipolowych, o równej długości, otaczających dwu-sferyczny obiekt. Zadaniem autorów była maksymalizacja współczynnika absorpcji własnej (SAR) w wewnętrznym obiekcie, przy zachowaniu jego minimalnej wartości w zewnętrznej kuli. Zaproponowane podejście uwzględnia zmiany mocy i faz źródeł napięciowych zasilających poszczególne dipole szyku antenowego. Przedstawiona metoda może mieć olbrzymi wpływ na zlokalizowane grzanie guza podczas terapii ciepłem. (**Optymalizacja współczynnika SAR dla szyku z wieloma antenami dipolowymi pod kątem hipertermii miejscowej**)

**Keywords:** dipole antenna, phased array, optimization, specific absorption rate SAR, hyperthermia, FDTD method.

**Słowa kluczowe:** antena dipolowa, układ anten fazowanych, optymalizacja, współczynnik SAR, hipertermia, metoda FDTD.

## Introduction

Hyperthermia (HT) is defined as the phenomenon of natural or artificial increase in temperature of whole body or its specific parts such as tissues or organs [1]. A natural HT results from the impairment of the body's thermoregulatory system, which leads to defect the heat dissipation mechanism and, as a result, to heat accumulation in dysfunctional tissue. An artificial HT involves increasing the temperature in the target area to values 40–45°C [2] or even higher (so-called *thermal ablation*) [3], under the influence of external heat sources (eg. hot water or wax baths) or different EMF applicators including various-type solenoids, coils, antennas or their multi-element arrays [1, 2]. The main task of artificial HT is thermal damage of malignant cells that are more sensitive to high temperature than normal cells. The main reason for this is the fact that the cancer tissue is highly vascularized but the tumor vessels are unable to growth their cross-sections during heating and remove excess heat as in the case of healthy tissues. Therefore, the tumor heats up much faster than the surrounding tissues with the same power of RF or MV applicators [1].

The challenge of modern hyperthermia is to design such HT systems that selectively heat only cancerous tissue, keeping intact healthy tissues [4]. Developing research connected with the EM energy usage results in the emergence of novel radiating elements [5] that allow for constant and controlled EMF exposure conditions [6, 8]. Importantly, the use of high frequencies limits the area of tissue penetration [1]. Simultaneously, the combination of several probes in the antenna matrix allows to increase the EM energy accumulation in the target volume [9]. By utilizing several EMF sources with the appropriate power, amplitude and phase control of the power supply signals, the required heat focusing within the deep-seated tumors can be achieved [10, 11]. For better targeting the EM energy on treated tissue the hybrid wideband multichannel HT systems [12] may be used. Furthermore, the multi-frequency field focusing devices can be applied to limit the so-called hot spots [13]. To prevent superficial tissues overheating, the appropriate frequency and number of applicators can be employed [12]. According to bioheat equation, the requested temperature levels of given tissue are connected with corresponding specific absorption rate (SAR) values [14]. Very often, for locoregional tissue heating the single dipole antenna [6], their arrays [15], as well as more complex antenna matrixes [9, 11, 13, 16] are successfully utilized.

The current work presents the concept of optimizing the 16-dipole-antenna array by means of powers and phases of individual dipoles occurring in the antenna matrix based on the SAR maximization in the target volume. This article is an extension of the previous publication [2].

## Model Description

In current work, the authors have investigated a multi-antenna array including 16 dipole applicators surrounding the tested object, as depicted in Fig. 1. Each dipole contained two arms of equal sizes (with length  $L_d/2 = 50$  mm and radius  $r_d = 1$  mm) and port placed between them, which is mimicking a sinusoidal voltage source with an internal resistance of 50 Ω. Such a system, with evenly spaced elements, forms the circle of radius  $R_a = 50$  mm centred in the origin of coordinate system  $S_1(0,0,0)$ . The analysed object includes two spheres with radii of  $R = 46$  mm and  $r = 5$  mm, respectively. What is important, the inner sphere is shifted relative to the outer one and its centre is set at the point  $S_2(25,5,0)$  mm.

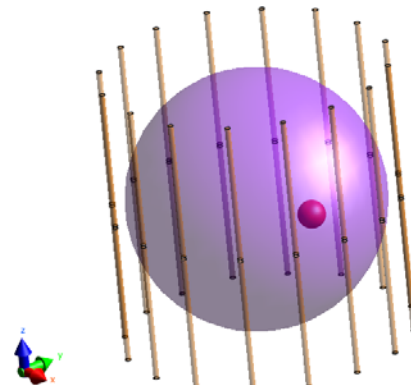


Fig. 1. Model of 16-dipole antenna array surrounding tested object

## Basic Equations

The outlined electro-thermal problem was numerically solved using the finite-difference time-domain (FDTD) method originally developed by K.S. Yee in 1966 [17]. This numerical approach is based on solving the Maxwell's equations in differential form, expressed as [2]:

$$(1) \quad \nabla \times \mathbf{H} = \frac{\partial}{\partial t} \epsilon_0 \epsilon_r \mathbf{E} + \sigma \mathbf{E}$$

$$(2) \quad \nabla \times \mathbf{E} = -\frac{\partial}{\partial t} \mu_0 \mu_r \mathbf{H} - \sigma_H \mathbf{H}$$

where  $\epsilon_r$  and  $\mu_r$  accordingly mean the relative permittivity and permeability of a medium. Moreover,  $\epsilon_0 = 8.85 \cdot 10^{-12}$  F/m and  $\mu_0 = 4\pi \cdot 10^{-7}$  H/m stand for the electric and magnetic constants, respectively. In addition,  $\sigma$  [S/m] and  $\sigma_H$  [ $\Omega$ /m] are conductivities that represent the electrical and magnetic losses occurring for proposed allocation of electric and magnetic fields. In the FDTD method, individual components of electric and magnetic field vectors ( $\mathbf{E}$  and  $\mathbf{H}$ ) are positioned in Cartesian coordinate system ( $x, y, z$ ) on the shifted Cubic grids and discretized by means approximation of the second order, which leads to the formulation of Maxwell's equations in scalar form with finite differences [18]:

$$(3) \quad \frac{\partial F(i, j, k, n)}{\partial x} = \frac{F^n(i+1/2, j, k, n) - F^n(i-1/2, j, k, n)}{\Delta x} + O[(\Delta x)^2]$$

$$(4) \quad \frac{\partial F(i, j, k, n)}{\partial t} = \frac{F^{n+1/2}(i, j, k) - F^{n-1/2}(i, j, k)}{\Delta t} + O[(\Delta t)^2]$$

where  $F_n$  represents the components of  $\mathbf{E}$  and  $\mathbf{H}$  vectors in discrete time  $t = n \cdot \Delta t$ . Moreover,  $i, j, k$  stand for the spatial indexes, and  $n$  is a temporal index.  $\Delta t$  denotes a time step,  $O[(\Delta x)^2]$ ,  $O[(\Delta y)^2]$ ,  $O[(\Delta z)^2]$  and  $O[(\Delta t)^2]$  express the error terms, and  $\Delta x, \Delta y, \Delta z$  are space increments along the axes.

In the field of electromagnetic dosimetry, the parameter, which determines an energy amount absorbed by biological systems and thus suitable thermal effect inside them, is the so-called specific absorption rate (SAR) [19]. It is used to estimate hazards coming from various RF and MV devices. At given point of the body  $\mathbf{r} = (x, y, z)$ , the local SAR value is calculated as proportion between the dissipated EM power and the density of the object, as defined below [20]:

$$(5) \quad \text{SAR}(\mathbf{r}) = \frac{d}{dt} \left( \frac{dW}{dm} \right) = \frac{d}{dt} \left( \frac{dW}{\rho dV} \right) = \frac{\sigma}{\rho} E^2 \sim \frac{dT}{dt}$$

where  $W$  [J] denotes the energy absorbed by the body,  $V$  [ $\text{m}^3$ ] is its volume,  $m$  [kg] – mass,  $\rho$  [ $\text{kg}/\text{m}^3$ ] – mass density, and  $t$  [s] means the exposure time. Additionally,  $E$  stands for the magnitude of electric field intensity induced at given location. What is more important, the SAR parameter can be averaged over given mass or volume of the object [21], and its value is reflected in the body temperature rise  $T$ .

The heat transfer within biological systems may be well evaluated with the Pennes bioheat equation [14, 22]:

$$(6) \quad \rho c \frac{\partial T}{\partial t} = \nabla \cdot (k \nabla T) + \rho Q_m + \rho \text{SAR}(\mathbf{r}) - \rho_b c_b \rho \omega (T - T_b)$$

where  $k$  [W/m/K] means a thermal conductivity,  $T$  [K] is the temperature, and  $c$  [J/kg/K] indicates specific heat of the object. Additionally, the Pennes model takes into account the so-called metabolic heat generation rate  $Q_m$  [W/kg] and the constant heat-transfer rate  $\rho_b c_b \rho \omega$  [W/m<sup>3</sup>/K], where  $\rho_b, c_b$  and  $T_b$  are accordingly the blood mass density, specific heat capacity of blood, and blood temperature. What is more,  $\omega$  [mL/min/kg] represents the blood perfusion rate in the tissue, and  $\rho \text{SAR}$  [W/m<sup>3</sup>] denotes the heat produced by the analysed 16-dipole antenna array. The heat flow with the surrounding environment is described using the convection phenomenon with the Robin boundary condition [2]:

$$(7) \quad \mathbf{n} \cdot (k \nabla T) = h(T - T_{\text{ext}})$$

where  $h$  [W/(m<sup>2</sup>·K)] stands for the heat transfer coefficient that is specified for the external surface of the body,  $T_{\text{ext}}$  is the ambient temperature of the air surrounding the object, and  $\mathbf{n}$  is the unit vector perpendicular to given body surface.

### Problem Optimization

For efficient HT treatment planning the main purpose should be to seek optimal phases and amplitudes of each dipole antenna within circular array for localized tumor heating [4, 11]. The aim of presented optimization problem was to specify powers  $P_i$  and phases  $\varphi_i$  of individual excitations  $e_i(t) = A_m \cos(2\pi f t + \varphi_i)$  [V] for each dipole antenna included in the matrix to minimize the value of SAR coefficient inside the outer sphere and at the same time to maximize it in the inner sphere. This can be successfully achieved by applying the objective function [2, 9, 23]:

$$(8) \quad \max \frac{\int_{\text{target}} w(\mathbf{r}) \text{SAR}(\mathbf{r}) dV}{\int_{\text{all targets}} w(\mathbf{r}) \text{SAR}(\mathbf{r}) dV}$$

or in the opposite form containing the frequency bandwidth of interest [12]. In current case a volume marked by term *target* represents the small sphere and term *all targets* was equivalent for both spheres. Importantly, in equation (8), the SAR coefficient is averaged over defined volumes of respectively the inner- and outer-sphere. Moreover, the total power of the 16-dipole antenna array was limited to 8 W to stabilize temperature in the target volume (small sphere) at 42°C. It was also assumed that phases of dipole voltage sources  $\varphi_i$  fluctuates in the range from 0° to 360°. In addition, all weigh factors in the system of dipole antennas were assumed as one. A various techniques of SAR optimization are reported in topic literature, including, among others, the optimal constrained power focusing [13], the time reversal method for power absorption focusing [11], E-field focusing [16], and many similar ones [10].

### Simulation Results

In the case of phased-array antenna systems the power dissipated in the body depends both on powers/amplitudes as well as phases of each antenna array sources. The assumptions made in the current simulation were as follows – each element of the 16-dipole antenna matrix was characterized in values:  $P_i = 1$  W,  $A_m = 1$  V, and  $\varphi_i = 0$ . What is important, the individual applicators worked at operating frequency equal to  $f = 1$  GHz. Furthermore, for mimicking the electro-thermal properties of human tissues for HT purpose, the outer sphere was linked with breast fat parameters, and the inner one – with muscle parameters. Table 1 compares the dielectric properties of human breast fat and muscle tissues to clearly show their strong dependence on exciting frequency [24]. In addition, other physical parameters fitted for the Pennes bioheat equation are gathered together in Table 2. In the FDTD method implementation it was assumed that relative permeability and magnetic conductivity have the following values  $\mu_r = 1$  and  $\sigma_H = 0$ . In presented model, the open boundary condition was applied on the outer surface of computational domain and the uniaxial perfectly matched layers (UPML) were applied for absorbing incident electromagnetic waves without any reflection. It was also assumed that initial temperature of both spheres has constant value  $T_0 = 309.75$  K = 36.6°C, which due to normal temperature of human body. Similar temperature level characterizes a blood  $T_b$  employed in the Pennes equation. What is more, all calculations were done for external temperature value (on the surface and outside of the big sphere) equal to  $T_{\text{ext}} = 25^\circ\text{C}$ , as well as the heat transfer coefficient applied as  $h = 5$  W/(m<sup>2</sup>·K). It worth noting that described optimization problem for SAR coefficient was solved by the FDTD engine available in the commercial software Sim4Life [7].

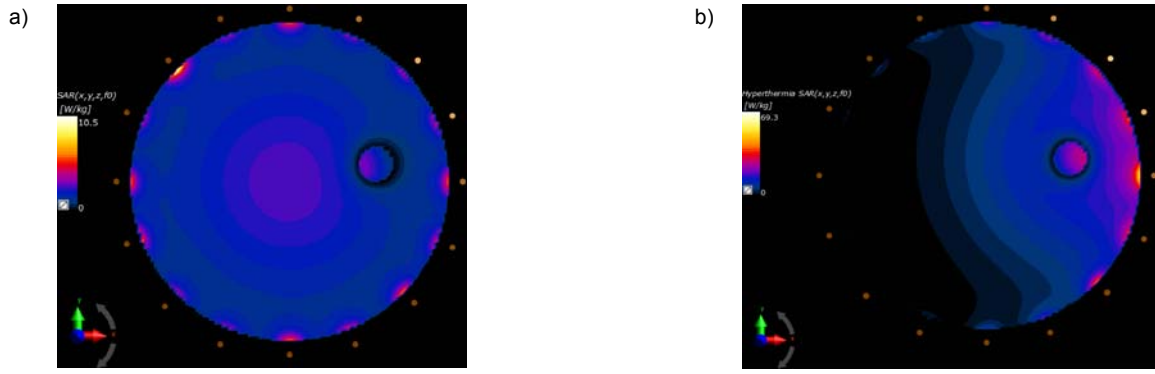


Fig.2. Distributions of SAR coefficient inside analysed object with 16-dipole antenna array: a) before optimization, and b) after optimization

Figure 2 compares the distributions of SAR parameter in the steady state for dipole antennas normalized to 1 W, both before (Fig. 2a) and after (Fig. 2b) employed optimization procedure. Charts in Fig. 3 show the optimized SAR distributions along the individual axes of the rectangular coordinate system  $(x, y, z)$ , referred to the small sphere centre. Similar distributions in the case of temperature are depicted in Fig. 4. Such curves seem to be symmetrical with respect to the centre of the inner sphere. The highest SAR and temperature levels were observed at the interface of two spherical objects, mainly for distributions along the antennas direction. The optimal results including powers of each matrix element and phases of dipole antennas excitations are listed in Table III. Importantly, the sum of all antennas powers is equal to 8 W, as assumed in current simulation. Fig. 5 illustrates a heat accumulation in a small sphere that is directly due to the increased SAR value in this area, according to the Pennes equation (6). Moreover, the temperature in the target region does not exceed therapeutic level  $42^{\circ}\text{C}$  after an exposure time 30 min, which creates good conditions for localized HT treatment.

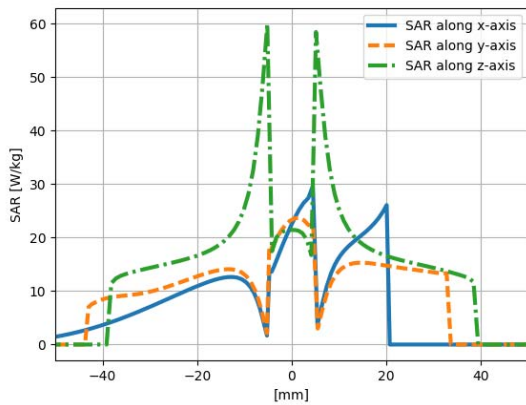


Fig.3. Optimized SAR distributions along respective axes of model related to the centre of a small sphere in the steady-state

Table 1. Dielectric properties for three example frequencies [24]

Tissue	Frequency		
	1 kHz	1 MHz	1 GHz
Blood	$\epsilon_r = 5\ 260$ $\sigma = 0.700\ \text{S/m}$	$\epsilon_r = 3\ 030$ $\sigma = 0.822\ \text{S/m}$	$\epsilon_r = 61.10$ $\sigma = 1.580\ \text{S/m}$
Breast fat	$\epsilon_r = 11\ 200$ $\sigma = 0.024\ \text{S/m}$	$\epsilon_r = 23.7$ $\sigma = 0.026\ \text{S/m}$	$\epsilon_r = 5.41$ $\sigma = 0.053\ \text{S/m}$
Muscle	$\epsilon_r = 435\ 000$ $\sigma = 0.321\ \text{S/m}$	$\epsilon_r = 1\ 840$ $\sigma = 0.503\ \text{S/m}$	$\epsilon_r = 54.80$ $\sigma = 0.978\ \text{S/m}$

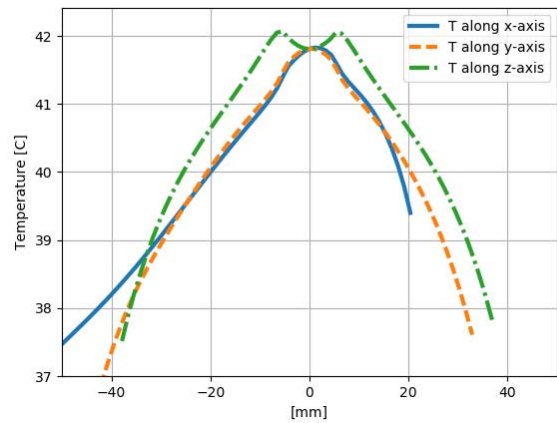


Fig.4. Temperature distributions along respective axes of model related to the centre of a small sphere in the steady-state

Table 2. The fitting parameters used for the Pennes equation [24]

Quantity	Blood	Breast fat	Muscle
$Q_m\ (\text{W/kg})$	0	0.728	0.906
$\rho_b, \rho\ (\text{kg/m}^3)$	1050	911	1090
$c_b, c\ (\text{J/kg/K})$	3617	2348	3421
$k\ (\text{W/m/K})$	0.5169	0.209	0.495
$\omega\ (\text{mL/min/kg})$	10\ 000	47	36.74
$\rho_b c_b \rho \omega\ (\text{W/m}^2/\text{K})$	$7.091 \cdot 10^5$	2892	2706

Table 3. The optimized parameters for the 16-dipole antenna array

Antenna No.	Power $P\ [\text{W}]$	Phase $\phi\ [^{\circ}]$
1	0.2916	171.2346
2	0.4850	171.6066
3	0.8870	135.3964
4	0.0659	170.5173
5	0.1036	-176.3429
6	0.6824	161.0660
7	0.7380	171.5533
8	0.0865	158.0882
9	0.3037	-179.3665
10	0.1453	-177.6521
11	0.6992	172.4827
12	0.6635	155.7106
13	0.3136	-168.2510
14	1.0012	118.0942
15	0.9270	169.4660
16	0.6065	180.0000

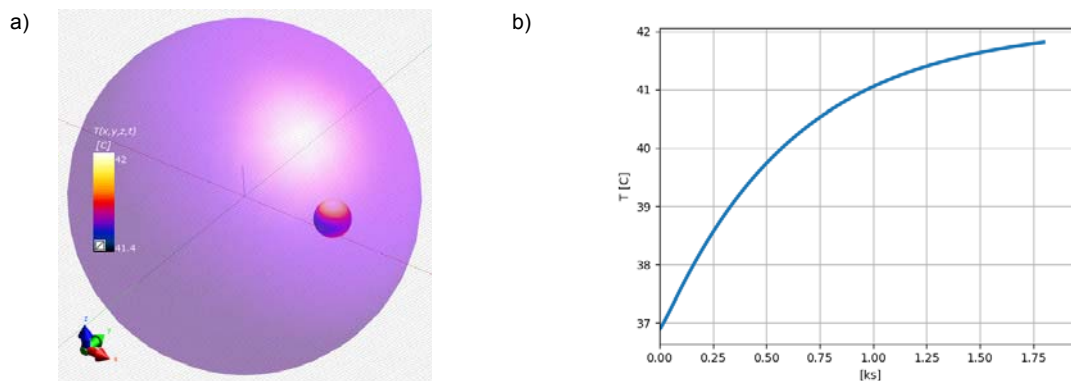


Fig.5. Temperature inside the objects in the case of: a) a steady-state, as well as b) transient analysis (point in the centre of inner sphere)

## Summary

The paper concerns the optimization procedure of multi-dipole antenna array surrounding the target object with regard to powers and phases of each matrix element. The main aim was to maximize the SAR concentration in region of interest, and to minimize in neighboring volume at the same time. Before the proposed optimization procedure, all dipole antennas were operated with the equal powers and zero phases, and the highest values of SAR coefficient were concentrated at the centre of outer sphere with low impact on the small one. The described algorithm allowed to estimate the optimal parameters of antennas for which a significant increase of SAR value inside the inner sphere appears. Simultaneously, it causes the temperature growth in target object to the therapeutic level, as clearly shown in performed simulation. Unfortunately, the external areas in direct proximity to the antennas were also heated, which is manifested by 'hot spots' occurrence, that are unavoidable without external body cooling. The considered optimization issue may be essential in localized tumor heat therapy.

**Authors:** dr inż. Piotr Gas, PhD, AGH University of Science and Technology, Department of Electrical and Power Engineering, al. Mickiewicza 30, 30-059 Krakow, E-mail: [piotr.gas@agh.edu.pl](mailto:piotr.gas@agh.edu.pl), dr inż. Arkadiusz Miaskowski, PhD, University of Life Sciences in Lublin, Department of Applied Mathematics and Computer Sciences, ul. Akademicka 13, 20-950 Lublin, Poland E-mail: [arek.miaskowski@up.lublin.pl](mailto:arek.miaskowski@up.lublin.pl).

## REFERENCES

- [1] Cala P., Bienkowski P., Antenna array for microwave ablation or hyperthermia working in the ISM 2.4 GHz band, *Przegląd Elektrotechniczny*, 94 (2018), No. 12, 238-241.
- [2] Miaskowski A., Gas P., Szczygiel M., Optimization of SAR coefficient for dipole antennas array with regard to local hyperthermia, in *2018 Applications of Electromagnetics in Modern Techniques and Medicine (PTZE)*, IEEE, (2018), [1-4]. Available at: <http://dx.doi.org/10.1109/PTZE.2018.8503175>
- [3] Karampatzakis A., et al., Heating characteristics of antenna arrays used in microwave ablation: A theoretical parametric study, *Computers in Biology and Medicine*, 43 (2013), No. 10, 1321-1327.
- [4] Fadeev A.M., et al., Thermometry system development for thermoradiotherapy of deep-seated tumours, *Journal of Physics: Conference Series*, 941 (2017), No. 1, Art. No. 012086, [1-6].
- [5] de Morais J.E.V., et al. Magneto Tuning of a Ferrite Dielectric Resonator Antenna Based on LiFe5O8 Matrix, *Journal of Electronic Materials*, 47 (2018), No. 7, 3829-3835.
- [6] Kodera S., Hirata A., Comparison of Thermal Response for RF Exposure in Human and Rat Models, *International Journal of Environmental Research and Public Health*, 15 (2018), No. 10, Art. No. 2320, [1-17].
- [7] <https://www.zurichmedtech.com/sim4life/> [12.10.2018]
- [8] Mazurek P.A., et al., The intensity of the electromagnetic fields in the coverage of GSM 900, GSM 1800 DECT, UMTS, WLAN in built-up areas, in *2018 Applications of Electromagnetics in Modern Techniques and Medicine (PTZE)*, IEEE, (2018), [1-4]. <http://dx.doi.org/10.1109/PTZE.2018.8503156>
- [9] Rijnen Z., et al., Quality and comfort in head and neck hyperthermia: a redesign according to clinical experience and simulation studies, *International Journal of Hyperthermia*, 31(2015), No. 8, 823-830.
- [10] Wiersma J., et al., A flexible optimization tool for hyperthermia treatments with RF phased array systems, *International Journal of Hyperthermia*, 18 (2002), No. 2, 73-85.
- [11] Takook P., et al., Performance Evaluation of Hyperthermia Applicators to Heat Deep-Seated Brain Tumors, *IEEE Journal of Electromagnetics, RF and Microwaves in Medicine and Biology*, 2 (2018), No. 1, 18-24.
- [12] Uddin N., Elshafiey I., Efficient energy localization for hybrid wideband hyperthermia treatment system, *International Journal of RF and Microwave Computer-Aided Engineering*, 28 (2018), No. 3, Art. No. e21238, [1-13].
- [13] Bellizzi G.G., et al., 3-D Field Intensity Shaping via Optimized Multi-Target Time Reversal, *IEEE Transactions on Antennas and Propagation*, 66 (2018), No. 8, 4380-4385.
- [14] Kok H.P., et al., Predictive value of simulated SAR and temperature for changes in measured temperature after phase-amplitude steering during locoregional hyperthermia treatments, *International Journal of Hyperthermia*, (2018), [1-10]. DOI: 10.1080/02656736.2018.1500720
- [15] Carrasco E., et al., Exposure assessment of portable wireless devices above 6 GHz, *Radiation Protection Dosimetry*, (2018), [1-8]. DOI: 10.1093/rpd/ncy177
- [16] Curto S., et al., Design and characterisation of a phased antenna array for intact breast hyperthermia, *International Journal of Hyperthermia*, 34 (2018), No. 3, 250-260.
- [17] Yee K.S., Numerical solution of initial boundary value problems involving Maxwell's equations in isotropic media, *IEEE Transactions on Antennas and Propagation*, AP14 (1966), 302-307.
- [18] Osaci M., Numerical Simulation Methods of Electromagnetic Field in Higher Education: Didactic Application with Graphical Interface for FDTD Method, *International Journal of Modern Education and Computer Science*, 10 (2018), No. 8, 1-10.
- [19] Ciosek K., Krawczyk A., Calculation of SAR in biological object of different parameters, *Przegląd Elektrotechniczny*, 83 (2007), No. 7-8, 93-95.
- [20] Miaskowski A., Gas P., and Krawczyk A., SAR Calculations for Titanium Bar-Implant Subjected to Microwave Radiation, *2016 17th International Conference Computational Problems of Electrical Engineering (CPEE)*, IEEE, (2016), [1-4]. Available at: <http://dx.doi.org/10.1109/CPEE.2016.7738726>
- [21] Corcoles J., et al., On the estimation of the worst-case implant-induced RF-heating in multi-channel MRI, *Physics in Medicine & Biology*, 62 (2017), No. 12, 4711-4727.
- [22] Pennes H.H., Analysis of Tissue and Arterial Blood Temperatures in the Resting Human Forearm, *Journal of Applied Physiology*, 85 (1998), No. 1, 5-34.
- [23] Capiello G., et al., Differential evolution optimization of the SAR distribution for head and neck hyperthermia, *IEEE Transactions on Biomedical Engineering*, 64 (2017), No. 8, 1875-1885.
- [24] Hasgall P.A., et al., IT'IS Database for thermal and electromagnetic parameters of biological tissues, Version 4.0, May 15th 2018.